



Consensus statement on thoracic radiology terminology in Portuguese used in Brazil and in Portugal

Bruno Hochhegger^{1,2,3}, Edson Marchiori⁴, Rosana Rodrigues⁵, Alexandre Mançano⁶, Dany Jasinowodolinski⁴, Rodrigo Caruso Chate⁷, Arthur Soares Souza Jr⁸, Alexandre Marchini Silva⁹, Márcio Sawamura¹⁰, Marcelo Furnari⁶, Cesar Araujo-Neto¹¹, Dante Escuissato¹², Rogerio Pinetti¹³, Luiz Felipe Nobre¹⁴, Danny Warszawiak¹⁵, Gilberto Szarf¹⁶, Gustavo Borges da Silva Telles⁷, Gustavo Meirelles¹⁷, Pablo Rydz Santana¹⁸, Viviane Antunes¹³, Julia Capobianco¹⁹, Israel Missrie¹⁹, Luciana Volpon Soares Souza⁸, Marcel Koenigkam Santos²⁰, Klaus Irion²¹, Isabel Duarte²², Rosana Santos²³, Eriquer Pinto²³, Diana Penha²³

1. Pontifícia Universidade Católica do Rio Grande do Sul – PUCRS – Porto Alegre (RS) Brasil.
2. Universidade Federal de Ciências da Saúde de Porto Alegre, Porto Alegre (RS) Brasil.
3. Thoracic Imaging Division, College of Medicine, University of Florida, Gainesville (FL) USA.
4. Universidade Federal do Rio de Janeiro – UFRJ – Rio de Janeiro (RJ) Brasil.
5. Universidade Federal do Rio Grande do Sul – UFRGS – Porto Alegre (RS) Brasil.
6. Sabin Medicina Diagnóstica, Brasília (DF) Brasil.
7. Hospital Israelita Albert Einstein, São Paulo (SP) Brasil.
8. Faculdade de Medicina de São José do Rio Preto, São José do Rio Preto (SP) Brasil.
9. Santa Casa de Misericórdia de São Paulo, São Paulo (SP) Brasil.
10. Universidade de São Paulo – USP – São Paulo (SP) Brasil.
11. Universidade Federal da Bahia – UFBA – Salvador (BA) Brasil.
12. Universidade Federal do Paraná – UFPR – Curitiba (PR) Brasil.
13. DASA Diagnósticos, São Paulo (SP) Brasil.
14. Universidade Federal de Santa Catarina, Florianópolis (SC) Brasil.
15. Diagnóstico Avançado por Imagem – DAPI – Curitiba (PR) Brasil.
16. Universidade Federal de São Paulo – Unifesp – São Paulo (SP) Brasil.
17. Aliar Diagnóstico por Imagem, São Paulo (SP) Brasil.
18. Hospital Beneficência Portuguesa de São Paulo, São Paulo (SP) Brasil.
19. Fleury Medicina e Saúde, São Paulo (SP) Brasil.
20. Faculdade de Medicina de Ribeirão Preto, Universidade de São Paulo – USP – Ribeirão Preto (SP) Brasil.
21. Manchester National Health Service, Manchester, United Kingdom.
22. Instituto Português de Oncologia de Lisboa Francisco Gentil, Lisboa, Portugal.
23. Universidade da Beira Interior, Covilhã, Portugal.

Submitted: 24 November 2020.
Accepted: 27 May 2021.

Correspondence to:

Bruno Hochhegger. Departamento de Radiologia, Pavilhão Pereira Filho, Irmandade Santa Casa de Misericórdia de Porto Alegre, Avenida Independência, 75, CEP 90020-160, Porto Alegre, RS, Brasil.
Tel.: 55 51 3214-8300. E-mail: brunochochegger@gmail.com
Financial support: None.

ABSTRACT

Effective communication among members of medical teams is an important factor for early and appropriate diagnosis. The terminology used in radiology reports appears in this context as an important link between radiologists and other members of the medical team. Therefore, heterogeneity in the use of terms in reports is an important but little discussed issue. This article is the result of an extensive review of nomenclature in thoracic radiology, including for the first time terms used in X-rays, CT, and MRI, conducted by radiologists from Brazil and Portugal. The objective of this review of medical terminology was to create a standardized language for medical professionals and multidisciplinary teams.

Keywords: Tomography, X-ray computed; Radiography; Magnetic resonance imaging; Terminology as topic.

INTRODUCTION

The objective of medical terminology is to provide standardized language for medical professionals and multidisciplinary teams. This terminology allows effective multidisciplinary medical communication, faster sharing of data on and discussion of clinical cases, and data integration in patient clinical records. In addition, it should be noted that appropriate language can help reduce communication errors and inadequate documentation, which ensures that medical teams can analyze patient processes with greater speed and accuracy and, thus, provide faster diagnosis and treatment.^(1,2)

In order to summarize recent evidence on imaging descriptors critically, 25 experts from Brazil and 3 experts from Portugal, all of whom are members of the Imaging Committee of the Brazilian Thoracic Association, were invited to develop the present consensus glossary. A panel of experts selected topics or questions related to the most significant changes in previously published concepts, including the terminology used in chest X-rays, CT, and MRI—terms that had not been addressed previously. Each invited expert was responsible for reviewing a topic or answering a question in this consensus glossary. In a second phase, 3 experts discussed and structured all texts submitted by the others, and, in a third phase, all experts reviewed and discussed the present recommendations. The present consensus statement brings an increase of more than 50% over previously published terminologies and includes terms used in chest X-rays, CT, and MRI.⁽²⁾

In thoracic radiology, the written radiology report is the most important and often the only instrument of communication between the radiologist and the requesting physician. The objective of the present consensus statement was to standardize the terminology used in reporting chest images in Portuguese used in Brazil (main

subtitle) and used in Portugal. When the two languages have different terms for the same topic, the term in Portuguese used in Portugal is identified as [PP]. Since the original document was written in Portuguese, the terms in this translated English version are alphabetized by the names of their corresponding terms in Portuguese, which are shown in parentheses.

ACINUS (ÁCINO)

The acinus is a structural anatomical unit of the lung. It is distal to a terminal bronchiole and contains alveolar ducts and alveoli. The acinus participates in gas exchange and is 6-10 mm in diameter. One secondary lobule contains between 3 and 25 acini. Acini are only visible on imaging when they accumulate (pathological) material, appearing as poorly defined nodular opacities on X-ray, CT, and MRI.⁽¹⁾

AIR TRAPPING OR GAS TRAPPING (APRISIONAMENTO AÉREO OU APRISIONAMENTO GASOSO [PP])

Air trapping is defined as retention of air (gas) in the distal airways and is visible on CT and MRI. It is best demonstrated in the expiratory phase and is seen as decreased attenuation of the lung parenchyma, showing lower-than-usual parenchymal density and lack of volume reduction (Figure 1).⁽¹⁻³⁾ It usually results from partial or complete airway obstruction or from focal abnormalities of lung compliance.⁽²⁾

ATELECTASIS OR COLLAPSE (ATELECTASIA OU COLAPSO)

Atelectasis is the term that describes reduced air volume in the affected lung. The most common mechanism of origin is airway obstruction with resorption of distal air. Atelectasis is characterized by volume loss, accompanied by opacity or increased attenuation, and displacement of fissures, bronchi, vessels, diaphragm, heart, or mediastinum (Figure 2). Passive atelectasis results from compression from pleural effusion or a mass. On imaging, atelectasis appears as an area of

hyperdensity (CT scans) or hyperintense signal (MRI scans) in the lung, that shows lung volume reduction, air bronchogram, and loss of vessel definition. It can be identified on chest X-rays, CT, and MRI.

ROUNDED ATELECTASIS (ATELECTASIA REDONDA)

Rounded atelectasis refers to the presence of focal lung collapse that accompanies a variety of conditions.⁽⁴⁾ It is typically associated with pleural disease, therefore being a relatively common finding in patients with asbestos exposure,⁽⁵⁾ in whom it is usually associated with a previous exudative pleural effusion or is the result of adjacent pleural fibrosis or diffuse pleural thickening.⁽⁴⁻⁷⁾ On axial imaging, rounded atelectasis appears as a round or oval mass that is located peripherally and abuts the pleural surface, which is usually thickened, with or without effusion. Rounded atelectasis is characteristically associated with a reduction in the volume of the involved lobe and with a curvilinear appearance of the vascular and bronchial structures adjacent to the lesion margins, forming the comet tail sign (Figure S1).^(2,5) Because rounded atelectasis represents collapsed lung parenchyma, it can show intense enhancement after contrast agent injection on both CT and MRI, a useful feature in differentiating it from lung neoplasms, which usually do not show such intense contrast agent uptake on contrast-enhanced imaging studies.

PARENCHYMAL BAND (BANDA PARENQUIMATOSA)

A parenchymal band is defined as an elongated linear opacity, 1-3 mm thick and up to 5 cm long, that can be seen in patients with fibrosis or other causes of interstitial thickening.⁽¹⁾ These bands are usually peripheral and often abut the pleural surface, which may be thickened and retracted at the site of contact. They can represent contiguous thickened interlobular septa, peribronchovascular fibrosis, coarse scars, or atelectasis associated with lung or pleural fibrosis of

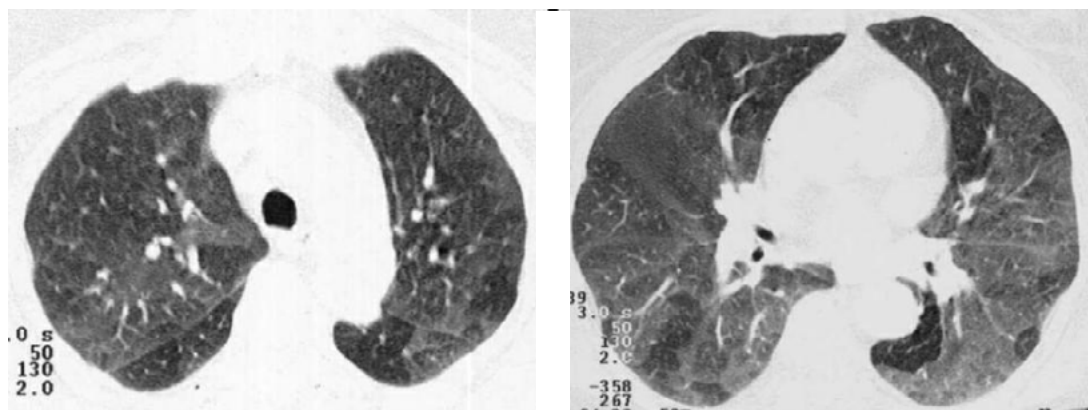


Figure 1. Axial CT scans with lung window settings acquired in the expiratory phase, revealing, in the posterior segments of the lower lobes, different parenchymal densities, with areas of decreased attenuation associated with air trapping due to small airway obstruction.

nonspecific cause (Figure S2).⁽⁵⁾ Parenchymal bands are most often seen in patients with asbestos exposure and sarcoidosis.

FUNGUS BALL (*BOLA FÚNGICA*)

A fungus ball is defined pathologically as a mass of intertwined hyphae, usually of an *Aspergillus* species, colonizing a cavity containing mucus, fibrin, and cellular debris. It usually occurs in a cavity from prior fibrocavitary disease (e.g., tuberculosis or sarcoidosis), but it occasionally occurs in cysts, bullae, and bronchi. A fungus ball may move to a dependent location when the patient changes position and may show an air crescent sign (Figure 3). A fungus ball may appear as heterogeneous sponge-like attenuation and foci of calcification on CT and MRI. A synonym is aspergilloma.⁽⁸⁾ See "Air crescent sign".

BULLA (*BOLHA*)

A bulla is defined pathologically as an airspace measuring more than 1 cm—and can be several centimeters—in diameter, demarcated by a thin wall that is no greater than 1 mm in thickness. A bulla is usually accompanied by emphysema and changes in the adjacent lung (See "Bullous emphysema"). On

X-rays, CT, and MRI, a bulla appears as a rounded focal hyperlucency or area of hypoattenuation, 1 cm or more in diameter, bounded by a thin wall (Figure 4). Multiple bullae are frequent and are associated with pulmonary emphysema (centrilobular and paraseptal).⁽⁵⁾

BRONCHOCELE (*BRONCOCELE OU BRONCOCELO [PP]*)

A bronchocele is defined pathologically as segmental bronchial dilatation, typically cylindrical and branching, that is completely or partially filled with secretions, usually mucoid ones. A bronchocele may be due either to obstructive disease, of congenital, tumoral, or foreign body etiology; or to non-obstructive disease, such as asthma, allergic bronchopulmonary aspergillosis, or cystic fibrosis. On X-rays, a bronchocele appears as an elongated opacity with branching morphology, being more evident in the central regions of the lung. On CT and MRI, a bronchocele appears as an elongated structure with cylindrical morphology, and can have a branching Y- or V-shaped appearance (Figure S3 and Figure 5). This appearance often resembles that of a "gloved finger". On CT, hypoattenuating lung parenchyma distal to the alteration, especially in cases of bronchial atresia due to reduced ventilation and perfusion, and increased attenuation within

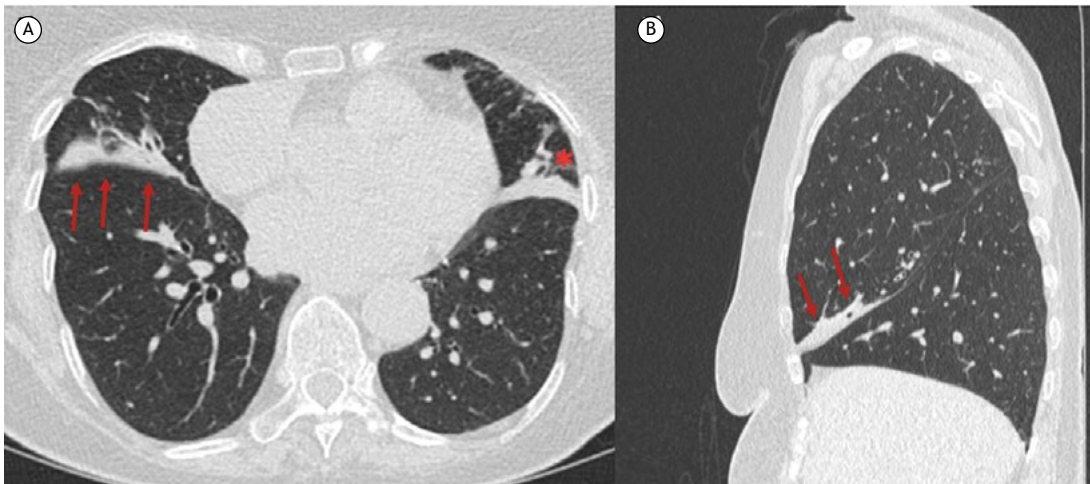


Figure 2. In A, an axial CT scan with lung window settings revealing atelectasis of the right middle lobe (arrows) and lingula (asterisk). In B, a coronal CT scan with lung window settings showing a slight displacement of the oblique fissure, bronchi, and adjacent vessels (arrows).

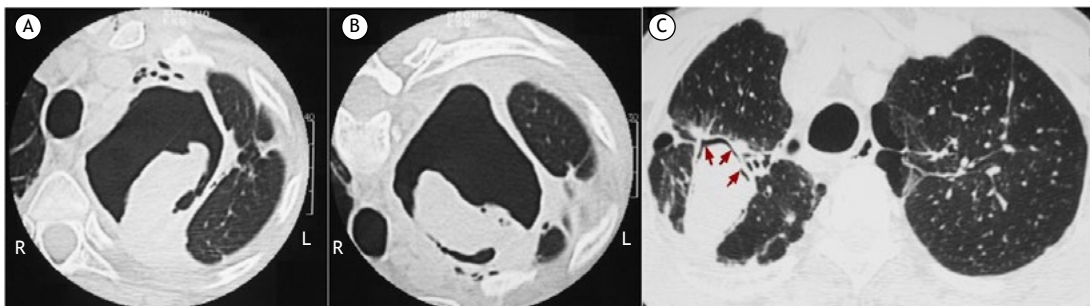


Figure 3. Axial CT scans with lung window settings acquired with the patient in the supine (A) and prone (B) positions, showing mobility of the fungus ball within a cavity in the left upper lobe. In C, an air crescent sign (arrows) within a cavity containing a fungus ball in the right upper lobe.

the bronchocele, which can be indicative of allergic bronchopulmonary aspergillosis, can be associated.⁽⁹⁾

AIR BRONCHOGRAM (*BRONCOGRAMA AÉREO*)

An air bronchogram is a branching air pattern within an area of increased attenuation of the lung parenchyma, reflecting air-filled bronchial structures in regions where there is no alveolar air, that is, regions of airspace filling (consolidation) or air absorption (atelectasis). On X-rays, an air bronchogram appears as a branching air pattern within an opacity. An X-ray finding of an air bronchogram indicates that the alteration is located in the lung parenchyma. On CT and MRI, an air bronchogram appears as an air-filled bronchial structure within a consolidation or area of

atelectasis of the lung parenchyma (Figure 6). When associated with atelectasis, an air bronchogram may indicate that there is no obstruction of proximal airways. Air bronchograms can occasionally be observed in adenocarcinomas and pulmonary lymphomas.⁽¹⁰⁾

BRONCHOLITH (*BRONCOLITO*)

A broncholith is defined pathologically as calcified or ossified material within the tracheobronchial tree. CT is superior to X-rays and MRI for diagnosis. The typical imaging appearance is of a focus of calcification adjacent to a bronchial wall or within a bronchus and with no soft tissue component, which distinguishes a broncholith from other lesions such as hamartomas or carcinoid tumors (Figure S4). Broncholiths are most common in the right upper and middle lobe bronchi, and can cause atelectasis, air trapping, and bronchiectasis because of the bronchial obstruction.⁽¹¹⁾

BRONCHIECTASIS (*BRONQUIECTASIA*)

Bronchiectasis is defined pathologically as irreversible focal or diffuse bronchial dilatation, usually secondary to inflammation and/or infection, bronchial obstruction, or congenital abnormality. X-ray findings can be nonspecific and include linear and/or reticular opacities, bronchial wall thickening, or even the demonstration of the bronchial dilatation. The CT diagnosis is made when the internal diameter of the bronchus is greater than the diameter of the adjacent artery (signet-ring sign); when there is a lack of bronchial tapering, defined as no change in bronchial diameter over 2 cm, distal to the bronchial bifurcation (tram-track appearance), and when bronchi are visible within 1 cm of the pleural surface (Figure 7). MRI can detect the same findings of bronchial dilatation that are seen on CT, but with less accuracy. Bronchiectasis is morphologically classified as cylindrical, when there is uniform bronchial dilatation; varicose, when there

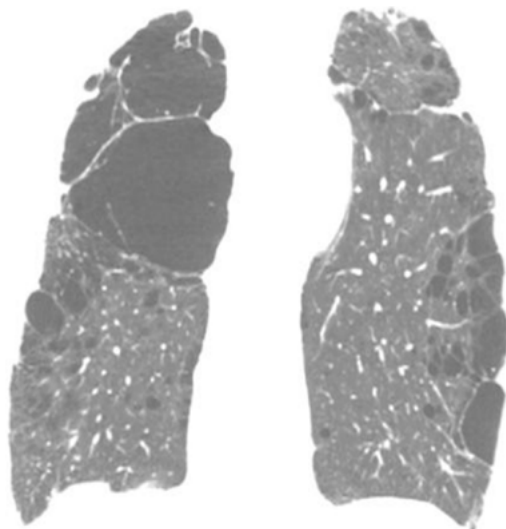


Figure 4. Coronal CT scans with lung window settings of a patient with centrilobular and paraseptal emphysema who has multiple bullae, the largest of which are located in the right lung apex.

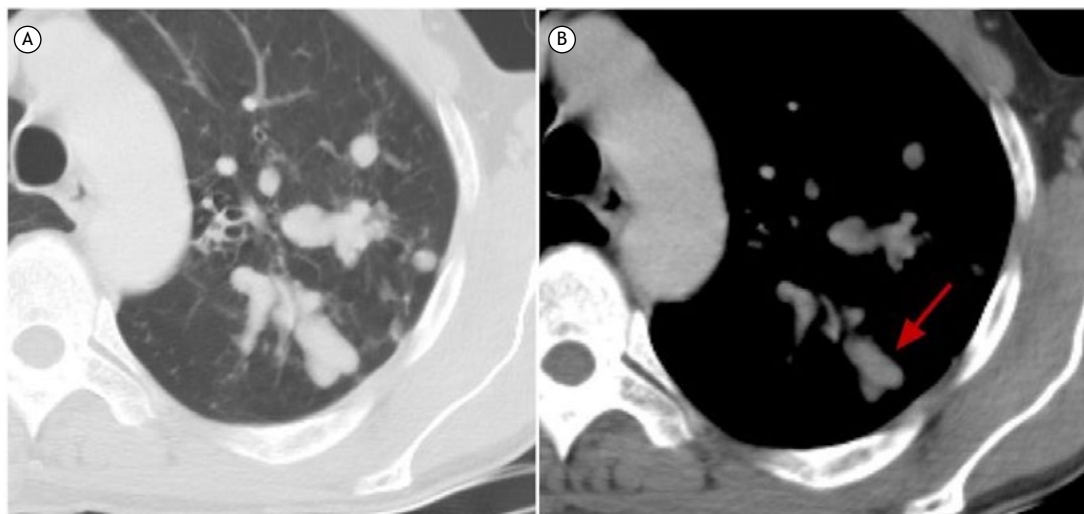


Figure 5. Axial CT scans of a patient with allergic bronchopulmonary aspergillosis (ABPA). In A, a CT scan with lung window settings showing bronchoceles. In B, a CT scan with mediastinal window settings showing increased attenuation (red arrow) within a bronchocele, suggesting the diagnosis of ABPA.

is irregular bronchial dilatation, with alternating areas of greater and smaller caliber; or cystic, when there is large focal dilatation, forming cysts.^(12,13)

BRONCHIOLECTASIS (*BRONQUIOLECTASIA*)

Bronchiolectasis is defined pathologically as dilatation of bronchioles. It is caused by inflammatory activity (therefore potentially reversible) or, more frequently, fibrosis, in which case it is referred to as "traction bronchiolectasis". Bronchioles differ from bronchi in that they have no cartilage or glands in their walls. The largest bronchioles are between 0.8 and 1.0 mm in diameter, with diameters gradually becoming smaller toward the level of the respiratory bronchioles

(the most distal ones, which have alveolar sacs on their walls), which are between 0.4 and 0.5 mm in diameter.^(4,12,13) Normal bronchioles are not visible on HRCT, the resolution limit of which allows visualization of bronchi that are up to 2-3 mm in internal diameter.⁽¹⁴⁾ When bronchioles are dilated and filled with secretions, they can be seen as centrilobular nodules or as a "tree-in-bud" pattern. Traction bronchiolectasis appears as small, cystic or tubular airspaces surrounded by fibrosis (Figure S5).^(1,15,16)

Traction bronchiolectasis is difficult to characterize on X-rays, and, when this happens, it is usually observed in the periphery of the lung bases. On CT, traction bronchiolectasis appears as bronchial dilatation that is

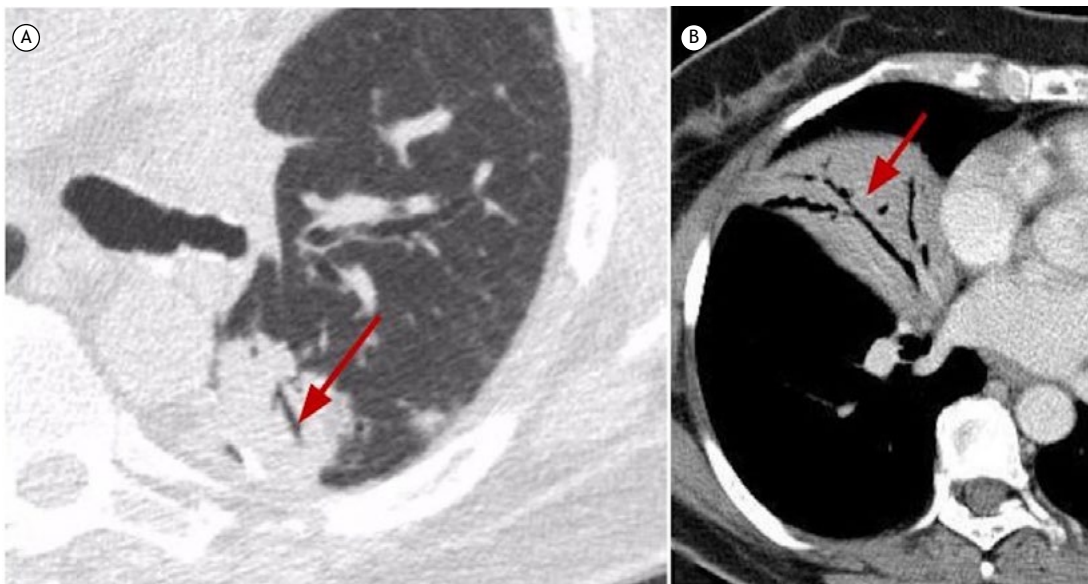


Figure 6. In A, an axial CT scan with lung window settings showing an air bronchogram (arrow) within a consolidation in the left lower lobe. In B, an axial CT scan with lung mediastinal window settings showing an air bronchogram (arrow) within a consolidation in the middle lobe.

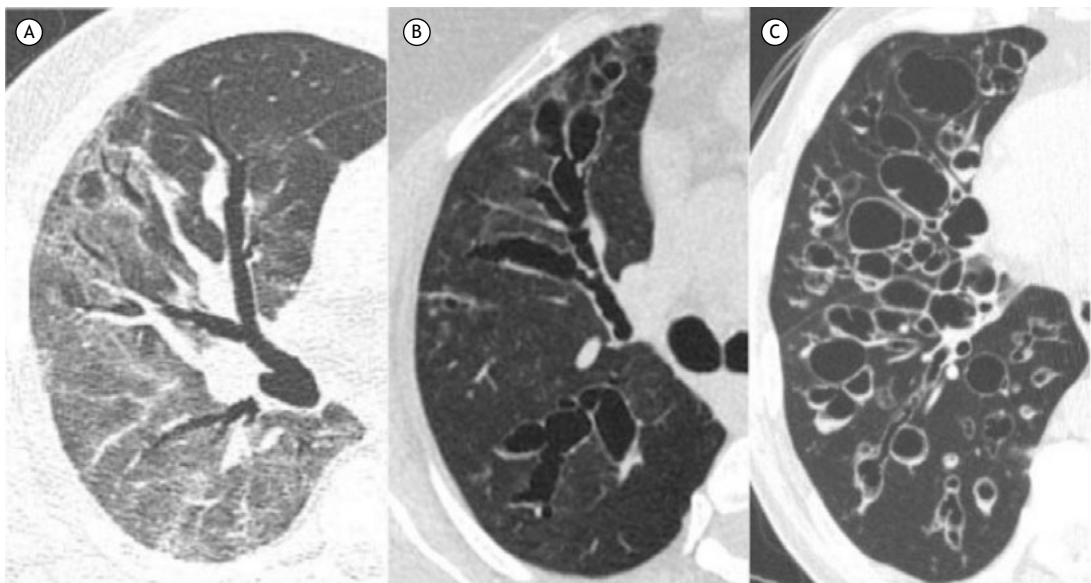


Figure 7. Axial CT scans with lung window settings showing cylindrical (A), varicose (B), and cystic (C) bronchiectasis.

tubular, cystic, or rounded in appearance, depending on the imaging axis. Traction bronchiolectasis is predominantly peripheral (juxtapleural), is smaller in internal diameter, and is associated with fibrosing interstitial lung changes (Figure S6). On MRI, traction bronchiolectasis is rarely visible and if so, it appears as a tubular structure of hypointense signal associated with areas of architectural distortion of the lung parenchyma.

CAVITY (CAVIDADE)

A cavity is defined pathologically as a gas-filled space, seen as a lucency or a low-attenuation area, within a mass, consolidation, or nodule.^(1,2) On X-rays, CT, and MRI, a cavity is an airspace measuring more than 1 cm (and can be several centimeters) in diameter, demarcated by a thick wall > 2 mm in thickness (Figure S7).⁽¹⁵⁾

CYST (CISTO OU QUISTO [PP])

A cyst is described pathologically as a round circumscribed space that is surrounded by an epithelial or fibrous wall of variable thickness.^(17,18) On chest X-rays, cysts are an infrequent and often inconclusive finding.^(17,18) On CT, a cyst appears as a round area of low attenuation in the lung parenchyma, with a well-defined interface with normal lung (Figure 8).^(17,18) Cyst walls are thin, being no greater than 2 mm in thickness. MRI is used for the study of mediastinal and thoracic non-air cystic lesions, playing an interesting role in their differential diagnosis and in determining hemorrhagic and fat components. Cysts usually contain air but occasionally contain fluid (e.g., bronchogenic cysts) or even solid material. Isolated pulmonary air cysts are common incidental findings and increase with age.^(17,18) The presence of five or more pulmonary cysts is used as a criterion for the investigation of cystic lung diseases.⁽⁵⁾ Cystic lung diseases usually present with multiple pulmonary cysts, often with increased lung volume, and include lymphangioleiomyomatosis, Langerhans cell histiocytosis, lymphocytic interstitial pneumonia, and Birt-Hogg-Dubé syndrome.^(17,18) However, there are fibrosing lung diseases that produce cysts, such as honeycomb cysts. See "Honeycombing".

ARCHITECTURAL DISTORTION (DISTRORÇÃO ARQUITETURAL)

Architectural distortion of the lung parenchyma is pathologically characterized by abnormal disorganized displacement of bronchi, vessels, fissures, or septa caused by diffuse or localized lung disease, particularly that associated with fibrosis and accompanied by volume loss.^(1,2) The term "architectural distortion" can be used in X-rays, CT, and MRI reports to describe regions where there is extensive anatomical disorganization that hinders exact anatomical recognition of structures (Figure S8).

EMPHYSEMA (ENFISEMA)

Emphysema is characterized pathologically by abnormal permanent enlargement of the airspaces distal to the

terminal bronchiole, accompanied by destruction of alveolar walls and without obvious fibrosis. The additional histological criterion of "absence of obvious fibrosis" has been questioned because some degree of interstitial fibrosis may be present in emphysema secondary to smoking. The traditional pathological classification of emphysema is based on the microscopic localization of disease within the acinus or secondary lobule. The main types of emphysema include centriacinar or centrilobular emphysema, paraseptal or distal acinar emphysema, and panacinar or panlobular emphysema.^(1,18-31) On CT, emphysema findings consist of areas of low attenuation, typically without visible walls.⁽²⁾

BULLOUS EMPHYSEMA (ENFISEMA BOLHOSO)

Bullous emphysema is not a specific histological entity but is rather the term for emphysema that is primarily characterized by the presence of a large bulla. Bullous emphysema is often associated with centrilobular and paraseptal emphysema (Figure S9).⁽¹⁸⁾ It is called giant bullous emphysema when the bullae occupy at least one third of the hemithorax and are asymmetrically located in the upper lobes, ranging from 1 to more than 20 cm in diameter.⁽¹⁹⁾ On CT, a bulla appears as a focal hypodense area, 1 cm or more in diameter, bounded by a thin wall that is no greater than 1 mm in thickness. It usually contains gas but may occasionally contain fluid.⁽¹⁾ Bullae that are less than 1 cm in diameter and are located within the visceral pleura or in the subpleural lung are called blebs. Apical blebs or vesicles are often responsible for primary spontaneous pneumothorax.⁽²⁰⁾

CENTRILOBULAR/CENTRIACINAR EMPHYSEMA (ENFISEMA CENTROLOBULAR/CENTROACINAR)

This type of emphysema pathologically corresponds to selective enlargement of elements in the central portion of the acinus, particularly the respiratory bronchioles and associated alveoli. The process primarily affects the upper lobes and the upper portion of the lower lobes, being strongly associated with smoking and chronic bronchitis. Inflammatory changes in the small airways are common, with plugging, mural infiltration, and fibrosis, which cause stenosis and airflow blockage, as well as distortion and destruction of the central portion of the acinus.⁽²¹⁻²³⁾ CT findings include multiple small rounded centrilobular areas of decreased parenchymal attenuation, without visible walls (Figure 9). A thin opaque rim can be seen in the transition zone between the emphysematous area and normal lung, because of compression of the adjacent parenchyma by the dilated airspace. Centrilobular arteries can often be seen within hypodense areas.⁽²²⁾ X-ray and MRI findings of centrilobular emphysema are only indirect, demonstrating increased lung volume, and are not diagnostically reliable.

INTERSTITIAL EMPHYSEMA (*ENFISEMA INTERSTITIAL*)

Interstitial emphysema is characterized by air dissecting within the lung interstitium and can be spontaneous or traumatic. It is most commonly seen in neonates receiving mechanical ventilation.⁽²⁴⁾ Interstitial emphysema is rarely identified on chest X-rays and may appear as intrapulmonary or subpleural cyst-like formations, radiolucent streaks extending to the mediastinum, and perivascular halos from air collections.⁽²²⁾ On CT, it appears as unilateral or bilateral diffuse focal collections of air, which can simulate cysts or bullae, located in the interstitium adjacent to the interlobular vessels, bronchi, and septa (Figure S10).^(25,26) X-ray and MRI findings of interstitial emphysema are nonspecific and are not diagnostically reliable.

PANACINAR OR PANLOBULAR EMPHYSEMA (*ENFISEMA PANACINAR OU PANLOBULAR*)

Panacinar emphysema is pathologically characterized by the enlargement of acinar airspaces, affecting the

structures from the respiratory bronchioles to the alveoli. All components of the secondary lobule are affected more or less uniformly.⁽²³⁾ This type of emphysema is associated with alpha-1 antitrypsin deficiency. Panacinar emphysema can be found in smokers, associated with centrilobular emphysema, and in intravenous drug users (chronic effect). In addition, it can be found around bronchoceles in patients with bronchial atresia. Chest X-rays may be normal in earlier disease stages. In more advanced stages, there is vascular distortion and rarefaction. Other findings include flattening of the diaphragm, increased anteroposterior chest diameter, and increased retrosternal space.⁽²⁷⁾ On CT, the lesions are homogeneously distributed, predominating in the lower lobes, and are characterized by a diffuse decrease in attenuation of the lung parenchyma with vascular rarefaction in the affected areas (Figure S11). Bronchiectasis may also be found. It may be difficult to differentiate between areas of normal lung parenchyma and areas of emphysema. Panacinar emphysema is indistinguishable from (constrictive) obliterative bronchiolitis.⁽²⁸⁾ MRI findings of panacinar



Figure 8. Axial (A) and coronal (B) CT scans with lung window settings revealing multiple pulmonary cysts in a female patient with lymphangioleiomyomatosis.

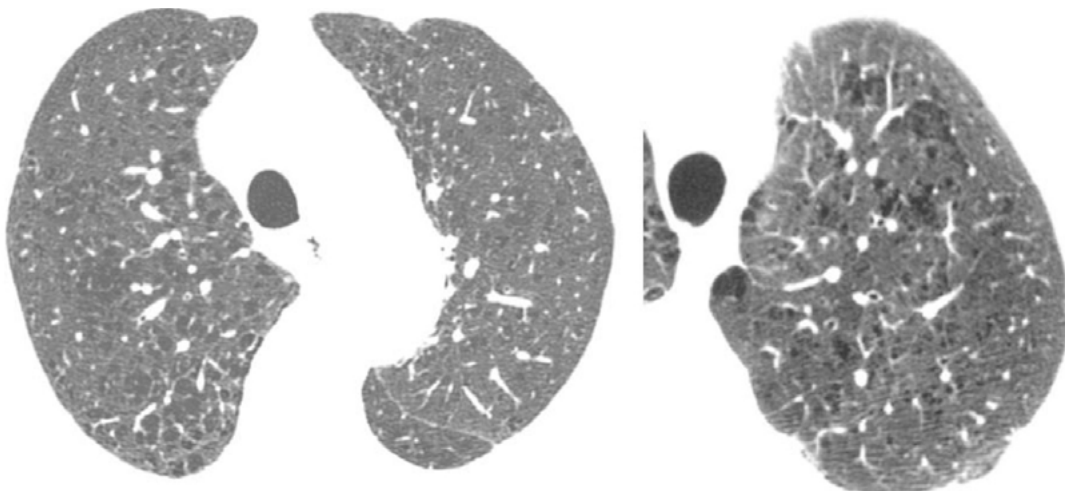


Figure 9. Axial CT scans with lung window settings revealing centrilobular emphysema in the upper lobes in a smoker.

emphysema are only indirect, demonstrating increased lung volume, and are not diagnostically reliable.

PARASEPTAL OR DISTAL ACINAR EMPHYSEMA (ENFISEMA PARASEPTAL OU ACINAR DISTAL)

This type of emphysema is pathologically characterized by permanent enlargement of the distal acinus, accompanied by destruction of alveolar ducts and sacs and with dilated alveoli in a subpleural location adjacent to the interlobular septa.⁽²⁹⁾ On chest X-rays, less severe forms of paraseptal emphysema are difficult to detect. Radiolucent thin-walled structures may be seen in the lung periphery.⁽²⁷⁾ On CT, subpleural and peribronchovascular cystic formations are seen, possibly separated by intact interlobular septa. The anterior and posterior portions of the upper lobes and the posterior portions of the lower lobes are most often affected. Bullae may be associated with this form of emphysema (Figure S12). The use of minimum-intensity projection reconstruction facilitates lesion detection.⁽³⁰⁾ MRI findings of paraseptal emphysema are nonspecific and are not diagnostically reliable.

AIRSPACES (ESPAÇOS AÉREOS)

The term "airspace" is a generic description that refers to the aerated portion of the lungs where there is gas exchange, that is, the respiratory bronchioles, alveolar ducts, and alveoli. This term excludes the purely conducting portion of the airways, from the trachea to the terminal bronchioles. Airspaces represent most of the normal lung. This term is usually used in conjunction with airspace-occupying diseases in which lung gas content is replaced by pathological products, either cells or fluid. In various lung diseases, the airspaces are occupied uniformly or areas of aerated lung are preserved within the lesion.^(2,32) On X-rays, the presence of air bronchograms may indicate the filling of the airspaces around the bronchi. On CT, lesions such as consolidations, masses, and nodules affect various lung compartments, including airspaces. Mostly, the term "airspace" is used when referring to airspace filling with pathological products or when there is aerated lung within those lesions (Figure S13). It is important to distinguish an airspace from a cavity, in which there is no gas content with no lung parenchyma.^(1,2,32) See "Cavity".

INTERLOBULAR SEPTAL THICKENING (ESPESSAMENTO DE SEPTOS INTERLOBULARES)

Interlobular septa are anatomically part of the peripheral interstitial framework of the lung, surround the secondary pulmonary lobule, and are composed of connective tissue, veins, and lymphatics. Normal interlobular septa are usually not visible on imaging. When thickened, they appear on X-rays as peripheral, thin linear opacities perpendicular to the pleural surface and are best visualized in the periphery of the lung

bases. They are also called Kerley B lines.^(1,2,32) On CT and MRI, they appear as peripheral/subpleural linear opacities perpendicular to the pleural surface, approximately 1.0-2.5 cm apart from each other. When the septa of several adjacent secondary pulmonary lobules are thickened, they may take on the appearance of polygonal arcades (Figure 10).^(4,18,30)

HONEYCOMBING (FAVEOLAMENTO)

Honeycombing is pathologically represented by acini dilated by fibrosis and forming cystic structures resulting from the collapse of neighboring acini. The cysts have thick, fibrous walls and are lined by metaplastic bronchiolar epithelium. On CT, honeycombing is seen as a cluster of cystic structures associated with reduced lung volume, typically has dimensions on the order of subcentimeters, and is usually subpleural. On MRI, the findings are similar, but the detection accuracy of MRI is lower than that of CT.⁽¹⁸⁾ Although honeycombing is represented by multiple layers of cysts in most cases, a cluster of two to three cysts together with other findings of fibrosis can be characterized as honeycombing.^(4,18) Honeycombing represents the late stage of various lung diseases, with complete loss of lung architecture, such as usual interstitial pneumonia and sarcoidosis (Figure S14).^(4,18)

FISSURE (FISSURA)

A fissure is anatomically defined as the infolding of visceral pleura that lines the outer surface of the lung and separates one lobe (or part of a lobe) from another. Each interlobar fissure is formed by the apposition of two layers of visceral pleura. In general, we can identify the major (or oblique) fissures, which separate the lower lobes from the other lobes, and the minor (or horizontal) fissure, which separates the middle lobe from the right upper lobe. Supernumerary fissures usually separate segments rather than lobes. Fissures may be incomplete. On imaging, fissures appear as linear opacities that correspond in position to the anatomic separation of pulmonary lobes or segments.^(1,33)

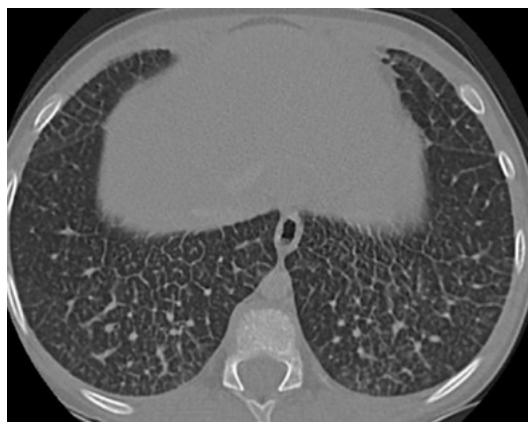


Figure 10. A CT scan with lung window settings revealing diffuse interlobular septal thickening, forming polygonal arcades.

INFILTRATE (INFILTRADO)

Infiltrate is considered an imprecise and nonspecific term often used to describe a region of pulmonary opacification, identified on X-rays, MRI, or CT, that is caused by airway or interstitial disease. Because infiltrate means different things to different people, it is considered a controversial term and is not recommended. We suggest that it be replaced by the term "opacity".⁽³⁴⁾

INTERFACE (INTERFACE)

Interface is an anatomical term to describe the boundary between two structures or tissues of different densities. When two thoracic structures of different radiological densities are juxtaposed, their boundaries are clearly defined. In imaging, this term is used only in HRCT studies of interstitial lung diseases. The interface sign is characterized by the presence of irregular interfaces between the lung and bronchi, vessels, and visceral pleura, being suggestive of interstitial thickening, usually associated with other changes, which together allow the diagnosis.^(33,35,36)

INTERSTITIUM (INTERSTÍCIO)

Interstitium is an anatomical term to describe the network of connective tissue that extends throughout the lungs and serves for their support. It comprises the following subdivisions: (a) axial (or bronchovascular) interstitium, which surrounds the bronchi, arteries, and veins from the hilum to the level of the respiratory bronchiole; (b) peripheral interstitium, which is the connective tissue contiguous with the pleural (subpleural) surfaces and interlobular septa; and (c) intralobular interstitium (also called acinar or parenchymal interstitium), which is a network of fine fibers interposed between the alveolar walls and the alveolar septal walls.^(1,36) The normal interstitium is not visible on imaging.

SUBPLEURAL CURVILINEAR LINE (LINHA CURVILÍNEA SUBPLEURAL)

A subpleural curvilinear line represents passive physiological compression of the dependent portion of the lung (e.g., of the posterior surface of the lung in patients in the supine position), which resolves after positional change. It may also be encountered in patients with pulmonary edema or fibrosis (Figure S15).⁽¹⁾ On CT and MRI, it appears as a thin curvilinear opacity, 1-3 mm in thickness, usually lying less than 1 cm from and parallel to the pleural surface.

SECONDARY PULMONARY LOBULE (LÓBULO PULMONAR SECUNDÁRIO)

Secondary pulmonary lobule is an anatomical term to describe the smallest unit of lung surrounded by connective tissue septa called interlobular septa. Each secondary pulmonary lobule is polyhedral in shape,

measures 1.0-2.5 cm in diameter, and contains a variable number of acini. The core of the lobule is composed of bronchioles and their accompanying pulmonary arterioles, lymphatics, and surrounding interstitium. Interlobular septa contain small pulmonary veins and lymphatics (Figure 10).^(37,38) Normal interlobular septa are not visible on imaging.

MASS (MASSA)

Mass is an imaging term to describe any expansile pulmonary, pleural, mediastinal, or chest wall lesion of soft tissue density, greater than 3 cm in diameter, and with at least partially defined contours, without regard to contour characteristics or content heterogeneity.^(1,39) The term can be used in X-rays, CT, and MRI. Pulmonary masses (Figure 11) are often associated with primary or metastatic neoplastic lesions; however, they may also represent inflammatory lesions, such as pseudotumors and organizing pneumonia (OP), or infectious lesions, such as tuberculomas and cryptococcomas.⁽⁴⁰⁾ Mediastinal masses can be classified by location in the mediastinum as anterior mediastinal (prevascular), middle mediastinal (visceral), or posterior mediastinal (paravertebral) masses to increase accuracy in differential diagnosis.⁽⁴¹⁾

MYCETOMA (MICETOMA)

Mycetomas characteristically represent a group of chronic subcutaneous infections caused by traumatic skin inoculation with material contaminated with actinomycetes, especially species of the genera *Nocardia*, *Streptomyces*, and *Actinomadura*, or true fungi (eumycetes), including the genera *Acremonium*, *Fusarium*, *Leptosphaeria*, and *Madurella*, resulting in actinomycetoma and eumycetoma, respectively.^(42,43) Mycetomas tend to invade adjacent tissues, forming nodules or masses with cavities and fistulous tracts, with purulent discharge containing grains composed of masses of hyphae and filaments. In most cases, they are located in the legs and can lead to deformities and fractures. Pulmonary and pleural involvement is rare.⁽⁴²⁾ When the lung is affected, the appearance is of consolidation with necrosis, and pleural effusion may be seen.⁽⁴³⁾ Mycetomas usually affect farm workers and are endemic in Latin America, India, and Africa.⁽⁴²⁻⁴⁶⁾ Mycetomas do not arise from colonization of preexisting pulmonary cavities; therefore, the use of the term "mycetoma" as a synonym for "fungus ball" should be avoided. See "Fungus ball".

NODULE (NÓDULO)

A nodule is defined as a focal opacity that is roughly rounded, or at least partially circumscribed; has soft tissue, fat tissue, or calcified tissue density; and measures up to 3 cm in diameter (opacities greater than 3 cm should be referred to as a "mass"; Figure 12).^(1,41) The term "nodule" can be used in X-rays, CT, and MRI. The term "small nodule" is suggested

for opacities up to 10 mm in mean diameter (average of the two largest diameters perpendicular to each other, preferably in the axial plane) or in diameter in another orthogonal plane if the opacities are larger in the longitudinal direction. Nodules larger than 10 mm should be measured at their largest and smallest orthogonal diameters. Nodules smaller than 3 mm require no formal measurement and can be termed micronodules.^(47,48) Nodules can be divided into solid nodules, when they completely obscure the contours of vessels and bronchial walls (Figure 12); pure ground-glass nodules, when they do not obscure the vascular margins or bronchial walls (Figure 12); and part-solid nodules, when there are areas of soft-tissue attenuation and areas of ground-glass attenuation (Figure 12).⁽⁴⁷⁾ In addition, nodules should be described according to their margins, morphology, and location. Perifissural nodules with elongated or polygonal morphology, for example, indicate benignity (pulmonary lymph nodes).⁽⁴⁸⁾ Multiple nodules should be classified according to their distribution (random nodular pattern, perilymphatic nodular pattern, or centrilobular nodular pattern, the latter with or without a tree-in-bud pattern). See "Mass", "Nodular pattern", "Miliary pattern", and "Tree-in-bud pattern".

OLIGEMIA (OLIGOEMIA)

Oligemia is a term that represents a focal, regional, or generalized reduction in pulmonary blood volume. Oligemia is demonstrated on CT and MRI but rarely on X-rays. It appears as a regional or widespread decrease in the caliber and number of pulmonary vessels, which is indicative of less than normal blood flow (Figure S16).^(1,2) Occasionally, areas of increased lung perfusion can simulate the appearance of ground-glass opacities, and, in differential diagnosis, it should be noted that there is a reduction in the number and caliber of the vessels in the regions of increased pulmonary lucency (Figure S17).⁽⁴⁹⁻⁵¹⁾

OPACITY (OPACIDADE)

Opacity is a generic term to describe any area that, because of its greater density, is at least partially distinguishable from the surrounding or superimposed structures. In chest X-ray studies, this term does not indicate the pathologic nature, size, or specific location of the abnormality. Opacities may either have a pulmonary, pleural, or chest wall origin or be caused by something external to the patient. On CT, pulmonary opacities may completely obscure the vascular structures and bronchial walls (as occurs in consolidation, solid nodules, and masses) or may appear as ground-glass attenuation (in which case the vascular structures and bronchial walls remain visible).^(1,2) The term "opacity" is not recommended for use in MRI. This term has some derivatives that merit discussion. See "Consolidation", "Ground-glass opacity", and "Mass".

GROUND-GLASS OPACITY (OPACIDADE EM VIDRO FOSCO OU DESPOLIDO [PP])

Ground-glass opacity is defined as an area of increased lung density (opacity) with attenuation that does not obscure underlying vascular structures.

On chest X-rays, ground-glass opacity appears as an area of hazy, low density, within which margins of pulmonary vessels may be indistinct. The considerable overlapping of structures on X-rays may lead to an incorrect interpretation of this finding, and the use of the term "ground-glass opacity" should therefore be avoided. On CT, ground-glass opacity appears as increased density of the lung parenchyma, with preservation of vascular and bronchial margins (Figure 13). It can represent interstitial thickening, partial filling of airspaces (with fluid, cells, and/or fibrosis), partial collapse of alveoli, increased capillary blood volume, or a combination of these mechanisms.^(52,53)

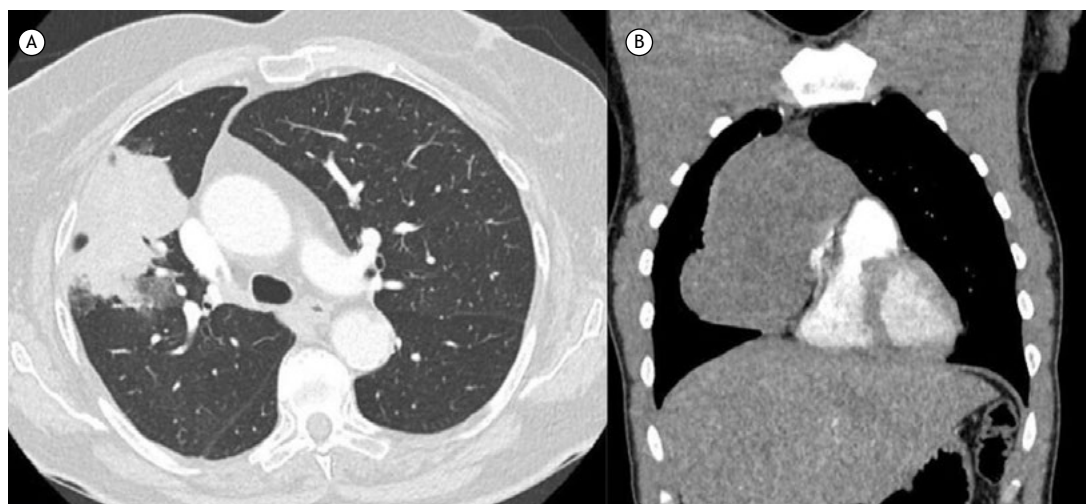


Figure 11. Axial CT scans with lung window settings. In A, a mass with lobulated contours in the anterior segment of the upper lobe of the right lung in a patient with lung adenocarcinoma. In B, an anterior mediastinal (prevascular) mass, with soft-tissue attenuation, in a patient with mediastinal seminoma.

Ground-glass opacity is less dense than and should be distinguished from consolidation, in which vessels are not identifiable within the affected area of lung (see "Consolidation"). Ground-glass opacity superimposed with intralobular lines and thickened interlobular septa results in a crazy-paving pattern (see "Crazy paving"). Ground-glass opacity with rounded/nodular morphology can be termed a subsolid nodule, which includes pure ground-glass nodules, that is, nonsolid nodules (Figure 13), or semisolid nodules, which contain soft-tissue density components.

On MRI, ground-glass opacity appears as an area of increased intensity on T2-weighted images, which is commonly observed in pathological processes, and this MRI finding highly correlates with CT findings of ground-glass opacity.⁽¹⁾

LINEAR OPACITY (OPACIDADE LINEAR)

On X-rays and CT, linear opacity appears as a thin elongated structure of greater density than the lung parenchyma (causing greater attenuation of the X-ray beam), with a number of etiologies. It is recommended whenever possible to use terms that are more specific, such as "parenchymal band", "linear atelectasis", or "interlobular septal thickening" (Figure S18).⁽²⁾

PARENCHYMAL OPACITY OR PARENCHYMAL OPACIFICATION (OPACIDADE PARENQUIMATOSA OU OPACIFICAÇÃO PARENQUIMATOSA)

On X-rays and CT, this type of opacity is characterized as any area of greater attenuation of the X-ray beam relative to the lung parenchyma. Increased attenuation of the lung parenchyma may or may not obscure the margins of vessels and bronchi (Figure 14). The term "consolidation" indicates loss of definition of the margins of vessels and bronchi (except for air bronchograms) within the opacity, whereas the term "ground-glass opacity" indicates a smaller increase in parenchymal attenuation, in which the definition of underlying structures is preserved.^(1,2,54,55)

DEPENDENT OPACITY (OPACIDADE PENDENTE)

On X-rays and CT, dependent opacity appears as increased density (greater attenuation of the X-ray beam) of the lung parenchyma in posterior subpleural regions (in the supine position) or anterior subpleural regions (in the prone position), representing positional atelectasis. It disappears with positional changes (Figure S18).^(1,2)

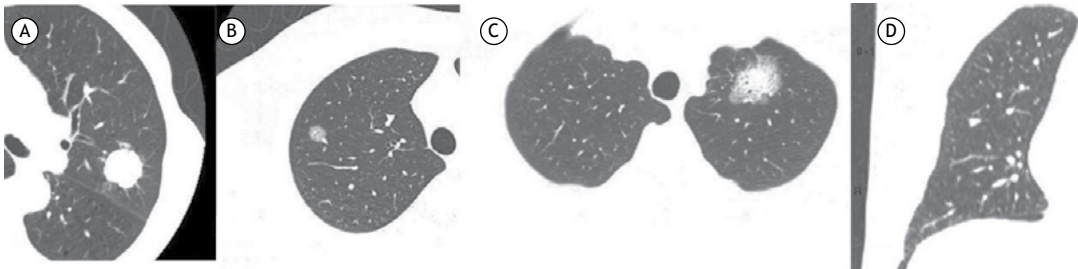


Figure 12. Axial CT scans with lung window settings. In A, a solid nodule with lobulated and spiculated margins in the apicoposterior segment of the upper lobe of the left lung. In B, a pure ground-glass nodule in the apical segment of the upper lobe of the right lung. In C, a mixed (part-solid, part ground-glass) nodule in the upper lobe of the left lung. In D, a perifissural nodule, polygonal in morphology, adjacent to the horizontal fissure of the right lung (pulmonary lymph node).

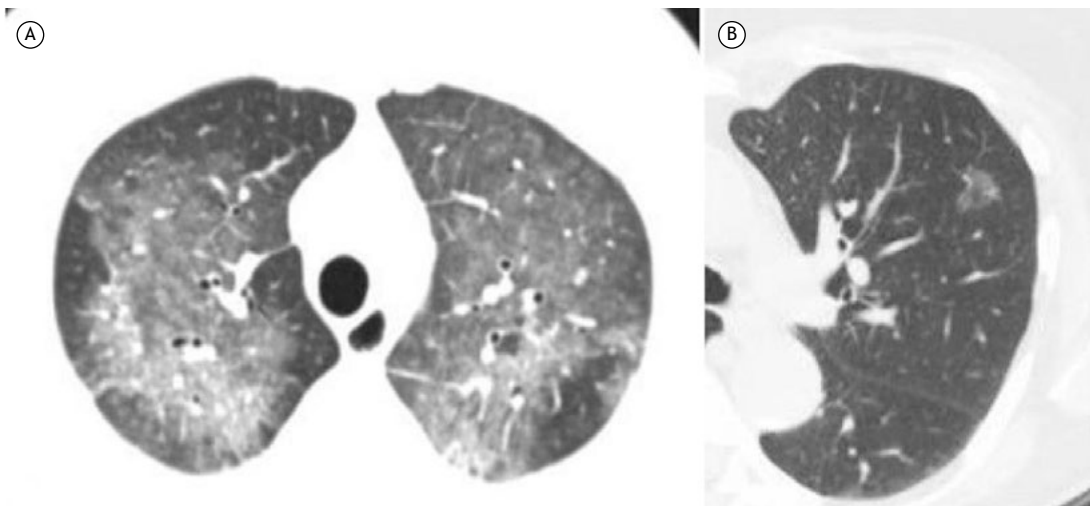


Figure 13. Axial CT scans with lung window settings demonstrating ground-glass opacities and predominant central distribution in both lungs in a patient with pulmonary edema (A) and revealing a ground-glass (subsolid) nodule that was diagnosed as lepidic growth adenocarcinoma (B).

CRAZY PAVING (PAVIMENTAÇÃO EM MOSAICO)

Crazy paving is a CT-specific term that describes a mixed pattern consisting of thickened interlobular septa and intralobular lines superimposed on a background of ground-glass opacity. It occurs in conditions involving the interstitium and the airspace. It is encountered in various diseases such as alveolar proteinosis, alveolar hemorrhage, ARDS, or infections, such as *Pneumocystis carinii* infection or the recent SARS-CoV-2 infection (Figure S19).^(56,57)

TREE-IN-BUD PATTERN (PADRÃO DE ÁRVORE EM BROTAMENTO OU EM BOTÃO [PP])

The term “tree-in-bud pattern” can be used in X-rays, CT, and MRI, and is defined as centrilobular branching opacities/nodules, with small nodularities at the extremities, that resemble a budding tree (Figure 15). This pattern results from the filling of centrilobular branching structures, whether the centrilobular bronchiole or artery. It reflects a broad spectrum of endo- and perilobular changes, including inflammation and exudation.^(1,58)

In most cases, this pattern represents dilated bronchioles filled with pathological material, although it may also be associated with infiltration of the peribronchial

connective tissue in the centrilobular vasculature or, occasionally, with dilatation or filling (e.g., intravascular metastases) of the centrilobular arteries.⁽⁵⁸⁾

MILIARY PATTERN (PADRÃO MILIAR)

A miliary pattern is an imaging finding on X-rays, CT, and MRI. It consists of nodules < 3 mm (micronodules) that are randomly and diffusely distributed and are uniform among themselves.⁽⁵⁹⁾ It is often a manifestation of hematogenous spread of tuberculosis and metastatic disease (Figure S20).^(1,2,60)

MOSAIC PERFUSION PATTERN (PADRÃO DE PERFUSÃO EM MOSAICO)

A mosaic perfusion pattern is a CT finding defined as a patchwork of areas of different attenuation. It results from small airways obliteration or occlusive vascular disease, both of which producing areas of oligemia (decreased attenuation) that are interspersed with areas of normally ventilated and perfused lung. In cases of obliterative small airways disease, expiratory CT enhances the parenchymal foci that are hypodense (decreased attenuation) because of the air-trapping component.^(1,2,61) The use of the term “mosaic attenuation” is no longer recommended because it increases the chances of misinterpretation

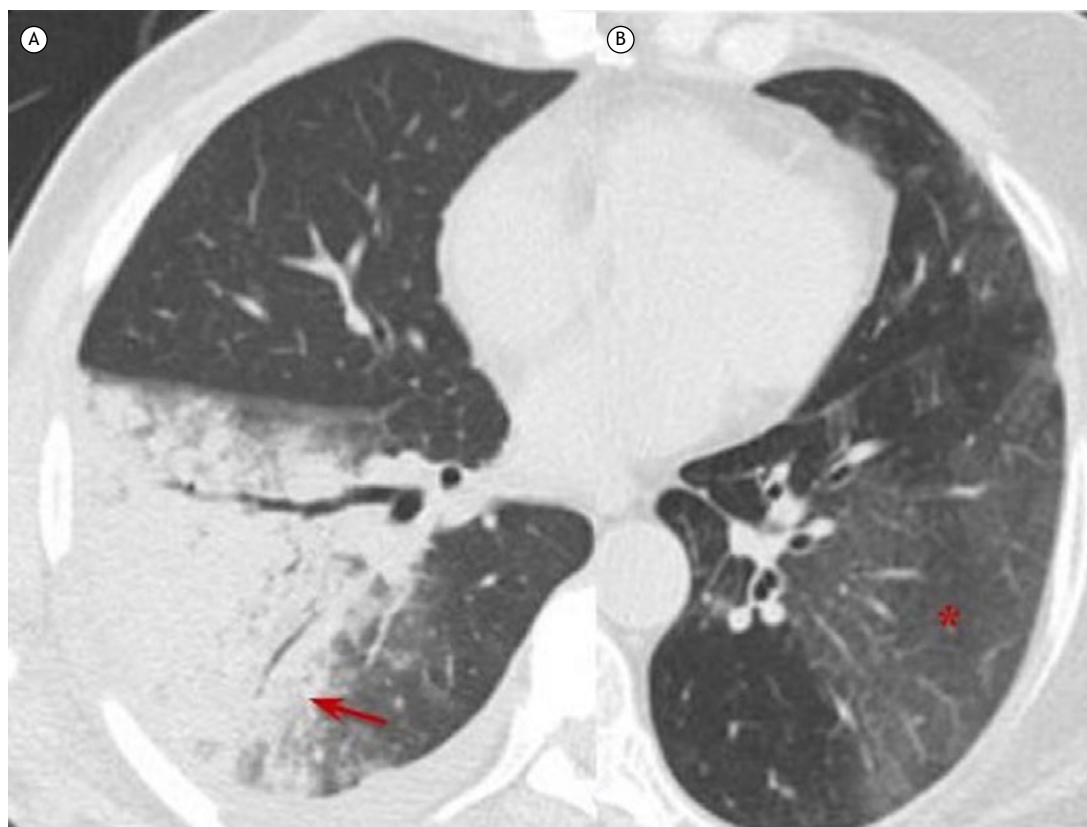


Figure 14. Axial CT scans with lung window settings showing parenchymal opacities that obliterate the contours of vessels and bronchi in the right lower lobe (arrow), indicating consolidation, together with an air bronchogram in the opacity (A), and parenchymal opacities preserving the contours of vessels and bronchi in the left lower lobe (asterisk), indicating ground-glass opacities (B).

regarding the term “mosaic perfusion”. The term “non-homogeneous ground-glass opacity” should be used instead of mosaic attenuation.

NODULAR PATTERN (PADRÃO NODULAR)

A nodular pattern refers to the presence of multiple round soft-tissue density pulmonary opacities less than 3 cm in diameter. This pattern can be demonstrated on X-rays, CT, and MRI. Small nodules (or micronodules) are those that are less than 1 cm in diameter. On the basis of their distribution in the lung parenchyma, they can be classified as perilymphatic, random, or centrilobular. A centrilobular distribution is characterized by nodules that occupy the central portion of the secondary pulmonary lobule and are within a few millimeters of the pleural surface and fissures but do not touch them. In general, this type of distribution is associated with bronchiolar diseases, arteriolar diseases, or peribronchovascular bundle diseases.⁽⁶⁰⁾ The nodular pattern is primarily seen in silicosis, hypersensitivity pneumonitis, and some forms of bronchiolitis. In most cases, the nodules found in hypersensitivity pneumonitis and bronchiolitis exhibit ground-glass attenuation.^(61,62)

PERILOBULAR PATTERN—PERILOBULAR OPACITIES, PERILOBULAR THICKENING (PADRÃO PERILOBULAR — OPACIDADES PERILOBULARES, ESPESSAMENTO PERILOBULAR)

A perilobular pattern represents involvement of the periphery of the secondary pulmonary lobule (i.e.,

the perilobular region) by variable histopathological substrates.^(63,64) On CT and MRI, it is seen as linear/curvilinear opacities surrounding interlobular septa, with the former being larger and less defined than the latter, and usually producing an appearance resembling a polygon or arch (Figure S21).⁽⁶³⁻⁶⁶⁾ The differential diagnosis includes OP, a pattern that is observed with differing frequency (22-57%) and represents collection of organizing inflammatory material in the periphery of the pulmonary lobule, with or without septal thickening.⁽⁶³⁻⁶⁵⁾ In OP, the perilobular pattern is often associated with other typical findings, such as consolidations, rather than being an isolated finding.⁽⁶⁶⁾

RETICULAR PATTERN (PADRÃO RETICULAR)

A reticular pattern represents involvement of the pulmonary interstitia by variable histopathological substrates. On X-rays, it appears as linear structures that are sometimes intertwined and are more easily seen in the periphery of the lung fields. On CT and MRI, it usually corresponds to inter- or intralobular septal thickening, but it can sometimes represent cysts whose walls appear as lines on X-rays (Figure S22). It is often, but not invariably, associated with fibrosing diseases, in which case signs of volume loss of the lung parenchyma are also observed.^(1,67)

PSEUDOPLAQUE (PSEUDOPLACA)

A pseudoplaque is an opacity contiguous with the visceral pleura, formed by coalescent small nodules.

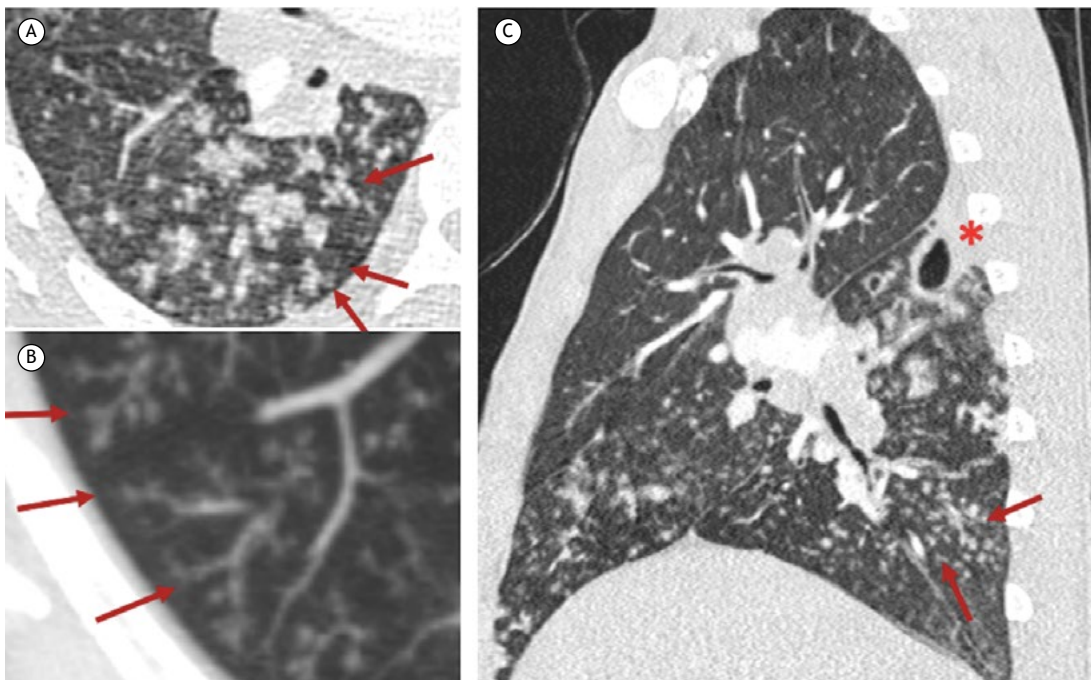


Figure 15. CT scans with lung window settings of a male patient with pulmonary tuberculosis. In A, an axial CT scan showing multiple centrilobular opacities with small nodules and branching structures (arrows). In B, maximum-intensity projection reconstruction demonstrating opacified structures that reflect endobronchial filling of the distal bronchioles (arrows). In C, a sagittal CT scan showing, in addition to centrilobular nodules and a tree-in-bud pattern (arrows), the presence of a cavity in the upper segment of the right lower lobe, which is a characteristic location for cavitation (asterisk) in pulmonary tuberculosis.

It simulates the appearance of a pleural plaque. This entity can be identified on CT and MRI and is encountered most commonly in sarcoidosis, silicosis, and coal workers' pneumoconiosis.⁽¹⁾

PLEURAL PLAQUE

A pleural plaque pathologically represents an elongated area of dense connective tissue on the pleural surface that appears as focal thickening on X-rays or more commonly on CT and MRI (Figure S23).^(1,68-70) It may be an incidental finding. However, when there are multiple pleural plaques, a differential diagnosis between asbestos exposure and sequelae of empyema/tuberculosis (usually unilateral and extensive) is necessary. Sometimes, pleural plaques are calcified, in which case they are more easily detected on X-rays as vertical linear structures parallel to the chest wall.

PNEUMATOCELE (PNEUMATOCELE)

A pneumatocele can be identified on X-rays, CT, and MRI, and is defined as a thin-walled (< 1 mm) and gas-filled rounded cystic structure that changes size within a short period of time (Figure S24). It results from a check-valve mechanism of airway obstruction. Occasionally, it may contain fluid. A pneumatocele usually resolves spontaneously. It is most often seen in children, in association with infectious processes, especially in children with pneumonia caused by *Staphylococcus* sp. and in immunocompromised children with pneumonia caused by *Pneumocystis jirovecii*.⁽⁷¹⁾ It can also be seen in preterm neonates with respiratory distress.⁽⁷²⁾

PSEUDOCAVITY (PSEUDOCAVIDADE)

Pseudocavity is a term used in CT to describe a round or oval, low-attenuation cystic area, usually < 1 cm in diameter, in lung nodules, masses, or areas of consolidation. A pseudocavity is sometimes difficult to differentiate from a pulmonary cavity. Pseudocavities can represent dilated or normal bronchi, areas of emphysema within a lesion, or areas of preserved lung parenchyma (Figures S25 and S26). The presence of a pseudocavity in nodules is often associated with adenocarcinoma and can be seen in pneumonia with necrotizing consolidation (Figure S26).⁽⁷¹⁻⁷³⁾

PNEUMOMEDIASTINUM (PNEUMOMEDIASTINO)

Pneumomediastinum is an imaging finding defined as the presence of air/gas in the mediastinum. Air or gas can reach the mediastinal spaces as a result of a sudden increase in intra-alveolar pressure, with consequent rupture of alveoli and tracking of gas along the peribronchovascular interstitium to the hilum and into the mediastinum. CT is the gold standard for diagnosis, which can also be made by X-rays (Figure S27). MRI is not used. Pneumomediastinum

may also be due to rupture of hollow organs, such as the esophagus, trachea, bronchi, or even the neck or abdominal cavity. Pneumomediastinum is often associated with pneumothorax.⁽⁷⁴⁾

PNEUMOTHORAX (PNEUMOTÓRAX)

Pneumothorax refers to the presence of air in the pleural space. It is usually classified as spontaneous, traumatic, diagnostic/iatrogenic, or tension, according to its etiology. It can be identified on X-rays, CT, and MRI (Figure S28). When its dimensions are significant (> 2 cm between the pleural surface and the pulmonary contour), pleural tube placement is indicated.^(1,2,74) In most cases, pneumothorax is caused by trauma such as rib fracture or penetrating chest trauma. Hypertensive pneumothorax is a medical emergency, because the air in the pleural cavity is under pressure, which causes associated vascular collapse and decreased venous return to the left atrium. Iatrogenic pneumothorax often results from thoracic procedures such as lung biopsy, central venous catheter insertion, or thoracic surgery.⁽⁷⁵⁾

TARGET SIGN (SINAL DO ALVO)

The target sign consists of a peripheral ring-shaped opacity in conjunction with a central nodular ground-glass opacity. The target sign can be demonstrated on CT and MRI. This finding was first described in association with SARS-CoV-2 pneumonia (Figure S29).⁽⁷⁶⁾ However, recent studies indicate that the etiopathogenesis of the target sign is similar to that of the reversed halo sign as a radiological sign of OP.⁽⁷⁷⁾

ARCH SIGN—PERILOBULAR SEPTAL THICKENING (SINAL DA ARCADEA — ESPESAMENTO SEPTAL PERILOBULAR)

The arch sign consists of an arch-shaped linear opacity with a perilobular distribution, around the secondary pulmonary lobule. This finding, like the target sign and the reversed halo sign, indicates OP (Figure S30).^(77,78) The arch sign can be demonstrated on CT and MRI.

SIGNET RING SIGN (SINAL DO ANEL DE SINETE)

The signet ring sign is composed of a ring-shaped opacity, representing a dilated bronchus in axial section, and a smaller adjacent opacity, representing its pulmonary artery, with the combination resembling a signet (or pearl) ring. This sign is a diagnostic CT feature of bronchiectasis (Figure S31). The signet ring sign can also be seen in diseases characterized by abnormal reduced pulmonary arterial flow, such as proximal interruption of the pulmonary artery or chronic pulmonary thromboembolism. Occasionally, a small vascular opacity abutting a bronchus is a bronchial, rather than a pulmonary, artery.⁽⁷⁹⁻⁸²⁾ See "Bronchiectasis".

AIR CRESCENT SIGN (SINAL DO CRESCENTE AÉREO)

The air crescent sign is a CT finding defined as a variable-sized, crescent- or half-moon-shaped collection of air in the periphery of a soft-tissue density nodule or mass (Figure S32). It is commonly described as an X-ray or CT finding of a fungus ball (aspergilloma), in which there is an air collection interposed between the wall of the preexisting cavity and the dependent intracavitary lesion. The air crescent sign has also been described in other diseases, such as angioinvasive pulmonary aspergillosis, lung abscess, lung cancer, and other fungal infections.⁽⁷²⁻⁷⁴⁾

HALO SIGN (SINAL DO HALO)

The halo sign is a nonspecific CT finding defined as a halo of ground-glass opacity surrounding a nodule or, less commonly, a mass or a rounded area of consolidation (Figure S33). In most cases, the halo of ground-glass opacity represents perinodular hemorrhage.⁽⁴⁾ In cases of angioinvasive aspergillosis (AIA), for example, the nodule represents pulmonary infarction secondary to fungal angioinvasion and the surrounding halo of ground-glass opacity represents perinodular alveolar hemorrhage. In other infectious processes, the halo sign represents perilesional inflammatory infiltration. In cases of adenocarcinoma, the halo sign represents tumor cell proliferation along the alveolar septa, with preservation of the lung architecture (lepidic growth).⁽¹⁾ The same features can be seen in some cases of metastatic adenocarcinoma (particularly in cases of adenocarcinoma originating from the gastrointestinal tract or pancreas). As an initial diagnostic approach, it is useful to determine patient immune status. In immunocompromised patients, the halo sign is most commonly due to infectious diseases, the most common being invasive fungal diseases, such as AIA. Therefore, in the presence of febrile neutropenia, especially in patients with hematologic malignancies and in bone marrow transplant recipients, AIA is the major cause of the halo sign.⁽¹⁾ In such cases, the halo sign is considered to constitute early evidence of AIA, warranting initiation of antifungal therapy before serologic test results are known.

REVERSED HALO SIGN (SINAL DO HALO INVERTIDO)

The reversed halo sign (RHS) is defined as a rounded area of ground-glass opacity surrounded by a ring of consolidation.⁽¹⁾ The RHS was first described as a sign specific for OP. Later studies identified RHS in a wide spectrum of infectious and noninfectious diseases.^(4,83-86) The most common infectious causes of RHS are tuberculosis, paracoccidioidomycosis, and invasive fungal diseases (invasive pulmonary aspergillosis and mucormycosis).⁽⁸⁷⁾ Among noninfectious diseases, both idiopathic or secondary OP is the most common cause. Other important causes are pulmonary infarction and sarcoidosis (Figure S34).⁽¹⁾ Although RHS is considered

a nonspecific sign, a careful analysis of its morphological characteristics can narrow the differential diagnosis, helping the attending physician to make a definitive diagnosis. Two imaging patterns should be taken into account in order to make the diagnosis more specific: the presence of nodules on the wall of and/or within the halo (nodular RHS); and a reticular pattern within the halo (reticular RHS). It should be borne in mind that these two patterns are not found in OP, which is the most common cause of RHS. These considerations are important because the treatment for these conditions is completely different.

BEADED SEPTUM SIGN—STRING-OF-BEADS SIGN/ROSARY SIGN/NODULAR SEPTAL THICKENING (SINAL DO SEPTO NODULAR – SINAL EM CONTAS/SINAL EM ROSÁRIO/ESPESSAMENTO SEPTAL NODULAR)

Interlobular septa surround the secondary pulmonary lobule and are composed of connective tissue, pulmonary veins, and lymphatics. Normal interlobular septa are usually not visible on radiological imaging but can sometimes be seen on HRCT, in which case they appear few in number, thin, and in the lung periphery.⁽³³⁾ Edema, inflammatory infiltrates, fibrosis, and neoplastic spread can lead to interlobular septal thickening, which can be smooth, irregular, or nodular. Nodular septal thickening is often associated with lymphangitic carcinomatosis or sarcoidosis, and, less often, it can also be seen in other lymphoproliferative disorders, in pneumoconiosis, and in amyloidosis.⁽¹⁾ On X-rays, it is difficult to determine whether the thickening is smooth or irregular/nodular, and the septal or reticular pattern of interstitial opacities is usually identified. Both CT and MRI allow us to identify nodular thickening of the interlobular septum, which takes on the appearance of a string of beads or rosary. In lymphangitic carcinomatosis, the beaded septum sign is most often focal and unilateral, being associated with unilateral hilar/mediastinal adenopathy and other suspicious changes in patients with a history of malignancy (Figure S35). In sarcoidosis, the beaded septum sign is most commonly bilateral and symmetric, seen predominantly in the middle and upper fields of the lungs, associated with bilateral hilar adenopathy, as well as in the right paratracheal stations. Sarcoidosis typically affects Black women between 20 and 40 years of age.⁽⁸⁸⁾

THORACOLITH/THORACOLITHIASIS (TORACOLITO/TORACOLITÍASE)

A thoracolith is defined as a small, free, and mobile structure/nodule, with or without calcification, in the pleural cavity (Figure S36). Thoracolithiasis is a rare benign condition characterized by the presence of one or more thoracoliths in the pleural cavity. The most characteristic radiological finding is mobility of the small structure/nodule, which can be demonstrated by sequential imaging or by changing patient position.

Thoracolithiasis is rarely symptomatic, being diagnosed on the basis of an incidental finding on X-rays or CT, and require no specific treatment, nor surgical resection.⁽⁸⁹⁾

reports, which should improve understanding of reports and result in better patient care.

FINAL CONSIDERATION

Although this article is not definitive, we believe that it can help radiologists to attempt standardization of

AUTHOR CONTRIBUTIONS

BH, CNA, and ASSJ: conception and planning of the study; and interpretation of results. All authors: drafting or revision of the preliminary and final versions; and approval of the final version.

REFERENCES

- Hansell DM, Bankier AA, MacMahon H, McLoud TC, Müller NL, Remy J. Fleischner Society: glossary of terms for thoracic imaging. *Radiology*. 2008;246(3):697-722. <https://doi.org/10.1148/radiol.2462070712>
- Silva CI, Marchiori E, Souza Júnior AS, Müller NL; Comissão de Imagem da Sociedade Brasileira de Pneumologia e Tisiologia. Illustrated Brazilian consensus of terms and fundamental patterns in chest CT scans. *J Bras Pneumol*. 2010;36(1):99-123. <https://doi.org/10.1590/s1806-37132010000100016>
- Arakawa H, Webb WR, McCowin M, Katsou G, Lee KN, Seitz RF. Inhomogeneous lung attenuation at thin-section CT: diagnostic value of expiratory scans. *Radiology*. 1998;206(1):89-94. <https://doi.org/10.1148/radiology.206.1.9423656>
- Woodring JH, Reed JC. Types and mechanisms of pulmonary atelectasis. *J Thorac Imaging*. 1996;11(2):92-108. <https://doi.org/10.1097/00005382-199621000-00002>
- Roach HD, Davies GJ, Attanoos R, Crane M, Adams H, Phillips S. Asbestos: when the dust settles an imaging review of asbestos-related disease. *Radiographics*. 2002;22 Spec No:S167-S184. https://doi.org/10.1148/radiographics.22.suppl_1.g02oc10s167
- Hillerdal G. Rounded atelectasis. Clinical experience with 74 patients. *Chest*. 1989;95(4):836-841. <https://doi.org/10.1378/chest.95.4.836>
- Gevenois PA, de Maertelaer V, Madani A, Winant C, Sergeant G, De Vuyst P. Asbestosis, pleural plaques and diffuse pleural thickening: three distinct benign responses to asbestos exposure. *Eur Respir J*. 1998;11(5):1021-1027. <https://doi.org/10.1183/09031936.98.11051021>
- Roberts CM, Citron KM, Strickland B. Intrathoracic aspergilloma: role of CT in diagnosis and treatment. *Radiology*. 1987;165(1):123-128. <https://doi.org/10.1148/radiology.165.1.3628758>
- Occelli A, Soize S, Ranc C, Giovannini-Chami L, Bailly C, Leloutre B, et al. Bronchocele density in cystic fibrosis as an indicator of allergic broncho-pulmonary aspergillosis: A preliminary study. *Eur J Radiol*. 2017;93:195-199. <https://doi.org/10.1016/j.ejrad.2017.05.047>
- Choi JA, Kim JH, Hong KT, Kim HS, Oh YW, Kang EY. CT bronchus sign in malignant solitary pulmonary lesions: value in the prediction of cell type. *Eur Radiol*. 2000;10(8):1304-1309. <https://doi.org/10.1007/s003300000315>
- Alshabani K, Ghosh S, Arrossi AV, Mehta AC. Broncholithiasis: A Review. *Chest*. 2019;156(3):445-455. <https://doi.org/10.1016/j.chest.2019.05.012>
- Barker AF. Bronchiectasis. *N Engl J Med*. 2002;346(18):1383-1393. <https://doi.org/10.1056/NEJMra012519>
- Cantin L, Bankier AA, Eisenberg RL. Bronchiectasis. *AJR Am J Roentgenol*. 2009;193(3):W158-W171. <https://doi.org/10.2214/AJR.09.3053>
- Akira M, Inoue Y, Kitaichi M, Yamamoto S, Arai T, Toyokawa K. Usual interstitial pneumonia and nonspecific interstitial pneumonia with and without concurrent emphysema: thin-section CT findings. *Radiology*. 2009;251(1):271-279. <https://doi.org/10.1148/radiol.2511080917>
- Souza Jr AS, Araujo Neto C, Jasinovodolinsky D, Marchiori E, Kavakama J, Irion KL, et al. Terminologia para a Descrição de Tomografia Computadorizada do Tórax. *Radiol Bras*. 2002;35(2):125-128. <https://doi.org/10.1590/S0100-39842002000200016>
- Funari MBG. Tomografia Computadorizada do Tórax Normal In: Funari MBG. Diagnóstico por Imagem das Doenças Torácicas. São Paulo: Guanabara Koogan; 2012. p. 87-106.
- Seaman DM, Meyer CA, Gilman MT, McCormack FX. Diffuse cystic lung disease at high-resolution CT. *AJR Am J Roentgenol*. 2011;196(6):1305-1311. <https://doi.org/10.2214/AJR.10.4420>
- Raouf S, Bondalapati P, Vydyla R, Ryu JH, Gupta N, Raouf S, et al. Cystic Lung Diseases: Algorithmic Approach. *Chest*. 2016;150(4):945-965. <https://doi.org/10.1016/j.chest.2016.04.026>
- Thurlbeck WN. Chronic airflow obstruction in lung disease. In: Bennington JL. Editor. Major Problems in Pathology, vol. 5. Philadelphia: Saunders; 1976. p. 221-302.
- Stern EJ, Webb WR, Weinacker A, Müller NL. Idiopathic giant bullous emphysema (vanishing lung syndrome): imaging findings in nine patients. *AJR Am J Roentgenol*. 1994;162(2):279-282. <https://doi.org/10.2214/ajr.162.2.8310909>
- Irion KL, Hochegger B, Marchiori E, Porto Nda S, Baldisserotto Sde V, Santana PR. Chest X-ray and computed tomography in the evaluation of pulmonary emphysema [Article in Portuguese]. *J Bras Pneumol*. 2007;33(6):720-732. <https://doi.org/10.1590/S1806-37132007000600017>
- Hruban RH, Meziene MA, Zerhouni EA, Khouri NF, Fishman EK, Wheeler PS, et al. High resolution computed tomography of inflation-fixed lungs. Pathologic-radiologic correlation of centrilobular emphysema. *Am Rev Respir Dis*. 1987;136(4):935-940. <https://doi.org/10.1164/ajrccm/136.4.935>
- Takahashi M, Fukuoka J, Nitta N, Takazakura R, Nagatani Y, Murakami Y, et al. Imaging of pulmonary emphysema: a pictorial review. *Int J Chron Obstruct Pulmon Dis*. 2008;3(2):193-204. <https://doi.org/10.2147/COPD.S2639>
- Sherren PB, Jovaisa T. Pulmonary interstitial emphysema presenting in a woman on the intensive care unit: case report and review of literature. *J Med Case Rep*. 2011;5:236. <https://doi.org/10.1186/1752-1947-5-236>
- Kemper AC, Steinberg KP, Stern EJ. Pulmonary interstitial emphysema: CT findings. *AJR Am J Roentgenol*. 1999;172(6):1642. <https://doi.org/10.2214/ajr.172.6.10350307>
- Donnelly LF, Lucaya J, Ozelame V, Frush DP, Strouse PJ, Sumner TE, et al. CT findings and temporal course of persistent pulmonary interstitial emphysema in neonates: a multiinstitutional study. *AJR Am J Roentgenol*. 2003;180(4):1129-1133. <https://doi.org/10.2214/ajr.180.4.1801129>
- Pipavath SN, Schmidt RA, Takasugi JE, Godwin JD. Chronic obstructive pulmonary disease: radiology-pathology correlation. *J Thorac Imaging*. 2009;24(3):171-180. <https://doi.org/10.1097/RTI.0b013e3181b32676>
- Litmanovich D, Boiselle PM, Bankier AA. CT of pulmonary emphysema—current status, challenges, and future directions. *Eur Radiol*. 2009;19(3):537-551. <https://doi.org/10.1007/s00330-008-1186-4>
- Araki T, Nishino M, Zazueta OE, Gao W, Dupuis J, Okajima Y, et al. Paraseptal emphysema: Prevalence and distribution on CT and association with interstitial lung abnormalities. *Eur J Radiol*. 2015;84(7):1413-1418. <https://doi.org/10.1016/j.ejrad.2015.03.010>
- Brauner M, Brillet P. Pathophysiological approach to infiltrative lung diseases on CT [Article in French]. *J Radiol*. 2009;90(11 Pt 2):1841-1853. [https://doi.org/10.1016/s0221-0363\(09\)73287-1](https://doi.org/10.1016/s0221-0363(09)73287-1)
- The definition of emphysema. Report of a National Heart, Lung, and Blood Institute, Division of Lung Diseases workshop. *Am Rev Respir Dis*. 1985;132(1):182-185.
- Webb WR, Muller NL, Naidich DP, editors. High-resolution CT of the lung. 4th ed. Philadelphia: Lippincott Williams & Wilkins; 2008.
- Tuddenham WJ. Glossary of terms for thoracic radiology: recommendations of the Nomenclature Committee of the Fleischner Society. *AJR Am J Roentgenol*. 1984;143(3):509-517. <https://doi.org/10.2214/ajr.143.3.509>

34. Patterson HS, Sponaugle DN. Is infiltrate a useful term in the interpretation of chest radiographs? Physician survey results. *Radiology*. 2005;235(1):5-8. <https://doi.org/10.1148/radiol.2351020759>
35. Naidich DP, Webb WR, Müller N, Vlahos I, Krinski GA, editors. *Computed tomography and magnetic resonance of the thorax*. 4th ed. Philadelphia: Lippincott Williams & Wilkins; 2007. p. 683.
36. Webb RW, Müller NL, Naidich DP. Airways diseases. In: Webb WR, Müller NL, Naidich DP, editors. *High-resolution CT of the lung*. 5th ed. Philadelphia: Lippincott Williams & Wilkins; 2014. p. 585-602.
37. Webb WR. Thin-section CT of the secondary pulmonary lobule: anatomy and the image—the 2004 Fleischner lecture. *Radiology*. 2006;239(2):322-338. <https://doi.org/10.1148/radiol.2392041968>
38. Webb WR, Müller NL, Naidich DP. Illustrated glossary of high-resolution computed tomography terms. In: Webb WR, Müller NL, Naidich DP, editors. *High-resolution CT of the lung*. 5th ed. Philadelphia: Lippincott Williams & Wilkins; 2014. p. 660-677.
39. MacMahon H, Naidich DP, Goo JM, Lee KS, Leung ANC, Mayo JR, et al Guidelines for Management of Incidental Pulmonary Nodules Detected on CT Images: From the Fleischner Society 2017. *Radiology*. 2017;284(1):228-243. <https://doi.org/10.1148/radiol.2017161659>
40. Giménez A, Franquet T, Prats R, Estrada P, Villalba J, Bagué S. Unusual primary lung tumors: a radiologic-pathologic overview. *Radiographics*. 2002;22(3):601-619. <https://doi.org/10.1148/radiographics.22.3.g02ma25601>
41. Carter BW, Benveniste MF, Madan R, Godoy MC, de Groot PM, Truong MT, et al. ITMIG Classification of Mediastinal Compartments and Multidisciplinary Approach to Mediastinal Masses. *Radiographics*. 2017;37(2):413-436. <https://doi.org/10.1148/rg.2017160095>
42. Ameen M, Arenas R. Developments in the management of mycetomas. *Clin Exp Dermatol*. 2009;34(1):1-7. <https://doi.org/10.1111/j.1365-2230.2008.03028.x>
43. Welsh O, Vera-Cabrera L, Salinas-Carmona MC. Mycetoma. *Clin Dermatol*. 2007;25(2):195-202. <https://doi.org/10.1016/j.clindermatol.2006.05.011>
44. Abd El-Bagi ME, Fahal AH. Mycetoma revisited. Incidence of various radiographic signs. *Saudi Med J*. 2009;30(4):529-533.
45. Muñoz-Hernández B, Noyola MC, Palma-Cortés G, Rosete DP, Galván MA, Manjarrez ME. Actinomycetoma in arm disseminated to lung with grains of *Nocardia brasiliensis* with peripheral filaments. *Mycopathologia*. 2009;168(1):37-40. <https://doi.org/10.1007/s11046-009-9189-5>
46. Lazac CS. Geographic distribution of mycetoma in Brazil [Article in Portuguese]. *An Bras Dermatol*. 1981;56(3):167-172.
47. Bankier AA, MacMahon H, Goo JM, Rubin GD, Schaefer-Prokop CM, Naidich DP. Recommendations for Measuring Pulmonary Nodules at CT: A Statement from the Fleischner Society. *Radiology*. 2017;285(2):584-600. <https://doi.org/10.1148/radiol.2017162894>
48. American College of Radiology (ACR) [homepage on the Internet. Reston, VA: ACR. Lung CT Screening Reporting & Data System (Lung-RADS). Available from: <https://www.acr.org/Clinical-Resources/Reporting-and-Data-Systems/Lung-Rads>
49. Martin KW, Sagel SS, Siegel BA. Mosaic oligemia simulating pulmonary infiltrates on CT. *AJR Am J Roentgenol*. 1986;147(4):670-673. <https://doi.org/10.2214/ajr.147.4.670>
50. Ameli-Renani S, Rahman F, Nair A, Ramsay L, Bacon JL, Weller A, et al. Dual-energy CT for imaging of pulmonary hypertension: challenges and opportunities. *Radiographics*. 2014; 34 (7): 1769-90. <https://doi.org/10.1148/rg.347130085>
51. Lu GM, Wu SY, Yeh, BM, Zhang LJ. Dual-energy CT for imaging of pulmonary hypertension: challenges and opportunities. *Radiographics*. 2014;34(7):1769-1790. <https://doi.org/10.1148/rg.347130085>
52. Remy-Jardin M, Remy J, Giraud F, Wattinne L, Gosselin B. Computed tomography assessment of ground-glass opacity: semiology and significance. *J Thorac Imaging*. 1993;8(4):249-264. <https://doi.org/10.1097/00005382-199323000-00001>
53. Remy-Jardin M, Giraud F, Remy J, Copin MC, Gosselin B, Duhamel A. Importance of ground-glass attenuation in chronic diffuse infiltrative lung disease: pathologic-CT correlation. *Radiology*. 1993;189(3):693-698. <https://doi.org/10.1148/radiology.189.3.8234692>
54. Barreto MM, Rafful PP, Rodrigues RS, Zanetti G, Hochegger B, Souza AS Jr, et al. Correlation between computed tomographic and magnetic resonance imaging findings of parenchymal lung diseases. *Eur J Radiol*. 2013;82(9):e492-e501. <https://doi.org/10.1016/j.ejrad.2013.04.037>
55. Leung AN, Miller RR, Müller NL. Parenchymal opacification in chronic infiltrative lung diseases: CT-pathologic correlation. *Radiology*. 1993;188(1):209-214. <https://doi.org/10.1148/radiology.188.1.8511299>
56. Rossi SE, Erasmus JJ, Volpacchio M, Franquet T, Castiglioni T, McAdams HP. "Crazy-paving" pattern at thin-section CT of the lungs: radiologic-pathologic overview. *Radiographics*. 2003;23(6):1509-1519. <https://doi.org/10.1148/rg.236035101>
57. El Homsy M, Chung M, Bernheim A, Jacobi A, King MJ, Lewis S, et al. Review of chest CT manifestations of COVID-19 infection. *Eur J Radiol Open*. 2020;7:100239. <https://doi.org/10.1016/j.ejro.2020.100239>
58. Franquet T, Giménez A, Prats R, Rodríguez-Arias JM, Rodríguez C. Thrombotic microangiopathy of pulmonary tumors: a vascular cause of tree-in-bud pattern on CT. *AJR Am J Roentgenol*. 2002;179(4):897-899. <https://doi.org/10.2214/ajr.179.4.1790897>
59. Marchiori E, Hochegger B, Zanetti G. Tree-in-bud pattern. *J Bras Pneumol*. 2017;43(6):407. <https://doi.org/10.1590/s1806-37562017000000303>
60. Marchiori E, Zanetti G, Hochegger B. Small interstitial nodules. *J Bras Pneumol*. 2015;41(3):250. <https://doi.org/10.1590/S1806-37132015000000059>
61. Almeida Junior JG, Marchiori E, Escuissato DL, Souza Jr AS, Gasparetto L, Nobre LF, et al. Pneumonite por hipersensibilidade (alveolite alérgica extrínseca): achados na tomografia computadorizada de alta resolução. *Rev Imagem*. 2003;25(4):231-237.
62. Marchiori E, Ferreira A, Saez F, Gabetto JM, Souza Jr AS, Escuissato DL, et al. Conglomerated masses of silicosis in sandblasters: high-resolution CT findings. *Eur J Radiol*. 2006;59(1):56-59. <https://doi.org/10.1016/j.ejrad.2006.01.015>
63. Ujita M, Renzoni EA, Veeraraghavan S, Wells AU, Hansell DM. Organizing pneumonia: peribubular pattern at thin-section CT. *Radiology*. 2004;232(3):757-761. <https://doi.org/10.1148/radiol.2323031059>
64. Johkoh T, Müller NL, Ichikado K, Nakamura H, Itoh H, Nagareda T. Peribubular pulmonary opacities: high-resolution CT findings and pathologic correlation. *J Thorac Imaging*. 1999;14(3):172-177. <https://doi.org/10.1097/00005382-199907000-00003>
65. Faria IM, Zanetti G, Barreto MM, Rodrigues RS, Araújo-Neto CA, Silva JL, et al. Organizing pneumonia: chest HRCT findings. *J Bras Pneumol*. 2015;41(3):231-237. <https://doi.org/10.1590/S1806-37132015000004544>
66. Torrealba JR, Fisher S, Kanne JP, Butt YM, Glazer C, Kershaw C, et al. Pathology-radiology correlation of common and uncommon computed tomographic patterns of organizing pneumonia. *Hum Pathol*. 2018;71:30-40. <https://doi.org/10.1016/j.humpath.2017.10.028>
67. Marten K. Reticular pattern in thin-section CT: from morphology to differential diagnosis [Article in German]. *Radiologe*. 2009;49(9):873-882. <https://doi.org/10.1007/s00117-009-1829-8>
68. Lynch DA, Gamsu G, Aberle DR. Conventional and high resolution computed tomography in the diagnosis of asbestos-related diseases. *Radiographics*. 1989;9(3):523-551. <https://doi.org/10.1148/radiographics.9.3.2727359>
69. Friedman AC, Fiel SB, Fisher MS, Radecki PD, Lev-Toaff AS, Caroline DF. Asbestos-related pleural disease and asbestosis: a comparison of CT and chest radiography. *AJR Am J Roentgenol*. 1988;150(2):269-275. <https://doi.org/10.2214/ajr.150.2.269>
70. Aberle DR, Gamsu G, Ray CS, Feuerstein IM. Asbestos-related pleural and parenchymal fibrosis: detection with high-resolution CT. *Radiology*. 1988;166(3):729-734. <https://doi.org/10.1148/radiology.166.3.3340770>
71. Kim TH, Kim SJ, Ryu YH, Chung SY, Seo JS, Kim YJ, et al. Differential CT features of infectious pneumonia versus bronchioloalveolar carcinoma (BAC) mimicking pneumonia. *Eur Radiol*. 2006;16(8):1763-1768. <https://doi.org/10.1007/s00330-005-0101-5>
72. Tailor TD, Schmidt RA, Eaton KD, Wood DE, Pipavath SN. The Pseudocavitation Sign of Lung Adenocarcinoma: A Distinguishing Feature and Imaging Biomarker of Lepidic Growth. *J Thorac Imaging*. 2015;30(5):308-313. <https://doi.org/10.1097/RTI.000000000000168>
73. Penha D, Pinto E, Taborda-Barata L, Irion K, Marchiori E. Lung cancer associated with cystic airspaces: a new radiological presentation of lung cancer. *J Bras Pneumol*. 2020;46(6):e20200156. <https://doi.org/10.36416/1806-3756/e20200156>

74. O'Connor AR, Morgan WE. Radiological review of pneumothorax. *BMJ*. 2005;330(7506):1493-1497. <https://doi.org/10.1136/bmj.330.7506.1493>
75. Sakai M, Hiyama T, Kuno H, Mori K, Saida T, Ishiguro T, et al. Thoracic abnormal air collections in patients in the intensive care unit: radiograph findings correlated with CT. *Insights Imaging*. 2020;11(1):35. <https://doi.org/10.1186/s13244-020-0838-z>
76. Müller CIS, Müller NL. Chest CT target sign in a couple with COVID-19 pneumonia. *Radiol Bras*. 2020;53(4):252-254. <https://doi.org/10.1590/0100-3984.2020.0089>
77. Marchiori E, Penha D, Nobre LF, Hochhegger B, Zanetti G. Differences and Similarities between the Double Halo Sign, the Chest CT Target Sign and the Reversed Halo Sign in Patients with COVID-19 Pneumonia. *Korean J Radiol*. 2021;22(4):672-676. <https://doi.org/10.3348/kjr.2020.1150>
78. Chiarenza A, Esposito Ultimo L, Falsaperla D, Travali M, Foti PV, Torrisi SE, et al. Chest imaging using signs, symbols, and naturalistic images: a practical guide for radiologists and non-radiologists. *Insights Imaging*. 2019;10(1):114. <https://doi.org/10.1186/s13244-019-0789-4>
79. Ouellette H. The signet ring sign. *Radiology*. 1999;212(1):67-68. <https://doi.org/10.1148/radiology.212.1.r99j2067>
80. Ryu JH, Swensen SJ. Cystic and cavitory lung diseases: focal and diffuse. *Mayo Clin Proc*. 2003;78(6):744-752. <https://doi.org/10.4065/78.6.744>
81. McGuinness G, Naidich DP, Leitman BS, McCauley DI. Bronchiectasis: CT evaluation. *AJR Am J Roentgenol*. 1993;160(2):253-259. <https://doi.org/10.2214/ajr.160.2.8424327>
82. Ryu DS, Spirn PW, Trotman-Dickenson B, Hunsaker A, Jung SM, Park MS, et al. HRCT findings of proximal interruption of the right pulmonary artery. *J Thorac Imaging*. 2004;19(3):171-175. <https://doi.org/10.1097/01.rti.0000130598.86945.b9>
83. Abramson S. The air crescent sign. *Radiology*. 2001;218(1):230-232. <https://doi.org/10.1148/radiology.218.1.r01ja19230>
84. Marshall GB, Farnquist BA, MacGregor JH, Burrowes PW. Signs in thoracic imaging. *J Thorac Imaging*. 2006;21(1):76-90. <https://doi.org/10.1097/01.rti.0000189192.70442.7a>
85. Wang LF, Chu H, Chen YM, Perng RP. Adenocarcinoma of the lung presenting as a mycetoma with an air crescent sign. *Chest*. 2007;131(4):1239-1242. <https://doi.org/10.1378/chest.06-1551>
86. Marchiori E, Zanetti G, Hochhegger B. Reversed halo sign. *J Bras Pneumol*. 2015;41(6):564. <https://doi.org/10.1590/s1806-37562015000000235>
87. Marchiori E, Hochhegger B, Zanetti G. Reversed halo sign in invasive fungal infections. *J Bras Pneumol*. 2016;42(3):232. <https://doi.org/10.1590/S1806-37562016000000119>
88. Ganeshan D, Menias CO, Lubner MG, Pickhardt PJ, Sandrasegaran K, Bhalla S. Sarcoidosis from Head to Toe: What the Radiologist Needs to Know. *Radiographics*. 2018;38(4):1180-1200. <https://doi.org/10.1148/rg.2018170157>
89. Escuissato DL, Zanetti G, Marchiori E. A mobile calcified nodule in the pleural cavity: thoracolithiasis. *J Bras Pneumol*. 2019;45(4):e20190113. <https://doi.org/10.1590/1806-3713/e20190113>



In the article "Consensus statement on thoracic radiology terminology in Portuguese used in Brazil and in Portugal", DOI number <http://dx.doi.org/10.36416/1806-3756/e20200595>, published in the *Jornal Brasileiro de Pneumologia*, 47(5):e20200595,2021, in the first page:

Where it reads:

Marcel Koeningan Santos

It should be read:

Marcel Koenigkam Santos